www.sciencetranslationalmedicine.org/cgi/content/full/5/211/211ra156/DC1

Supplementary Materials for

Restoration of the Unfolded Protein Response in Pancreatic β Cells Protects Mice Against Type 1 Diabetes

Feyza Engin, Alena Yermalovich, Truc Nguyen, Sarah Hummasti, Wenxian Fu, Decio L. Eizirik, Diane Mathis, Gökhan S. Hotamisligil*

*Corresponding author. E-mail: ghotamis@hsph.harvard.edu

Published 13 November 2013, *Sci. Transl. Med.* **5**, 211ra156 (2013)
DOI: 10.1126/scitranslmed.3006534

The PDF file includes:

Materials and Methods
Fig. S1. Specific alterations of the UPR mediators in the islets of NOD mice.
Fig. S2. Specific alterations of Glut2 and Keap1 expression in the islets of NOD mice.
Fig. S3. Dysregulation of the molecules critical in the UPR in the islets of male T1D patients.
Fig. S4. Immunophenotyping of splenocytes of NOD mice after TUDCA treatment.
Fig. S5. Immunophenotyping of pancreatic lymph nodes of NOD mice after TUDCA treatment.
Fig. S6. Deletion of ATF6 branch of the UPR in β cells in vivo.

Material and Methods

Glucose, and insulin tolerance tests, in vivo GSIS assay

Glucose tolerance tests (GTT) were performed in overnight fasted mice. Mice were given glucose (2 g/kg of body weight) intraperitoneally, followed by blood glucose measurements. Insulin tolerance tests (ITT) were performed after 6 hr day-time food withdrawal by intraperitoneally administration of 0.5 U/kg recombinant human regular insulin (Eli Lilly). *In vivo* glucose-stimulated insulin secretion (GSIS) tests were performed in mice following an overnight fast and by administration of 2g/kg glucose. Serum insulin levels were quantified by ELISA (Alpco, Ultrasensitive Mouse Insulin ELISA. NH, USA).

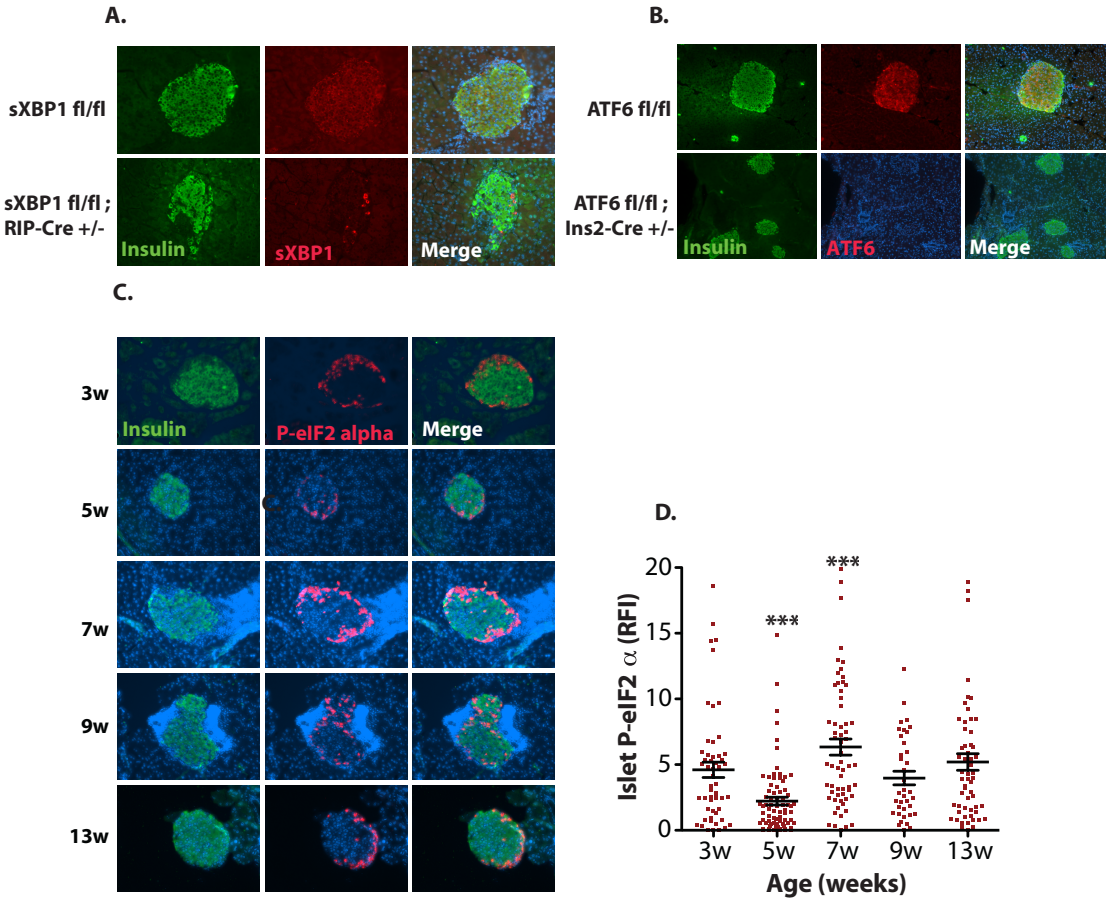

Fig. S1. Specific alterations of the UPR mediators in the islets of NOD mice.

A. Pancreatic sections from wild type and β-cell specific XBP1-deficient mice (sXBP1fl/fl, RIP-Cre) were stained with the anti-sXBP1 antibody to determine the specificity of the antibody. sXBP1 staining was only observed in non-insulin

producing cells. **B.** Pancreatic sections from wild type and β-cell specific ATF6-deficient mice (ATF6fl/fl, Ins2-Cre) were stained with the anti-ATF6 antibody to determine the specificity of the antibody. **C.** Female NOD mice (n=14 each group) were sacrificed at 3, 5, 7, 9 and 13 weeks of age. Immunofluorescence assay was done on the pancreas sections by performing co-stainings with phospho-eIF2α (red) and anti-insulin (green) antibodies. The cell nuclei were counterstained with DAPI (blue). **D.** Quantification of relative fluorescence intensity (RFI) for phospho-eIF2**α** was done using MATLAB® (20-30 islets/animal/time point). All data are represented as mean ± SEM, with statistical analysis performed by one-way ANOVA (****P<0.001*, **P<0.05*).

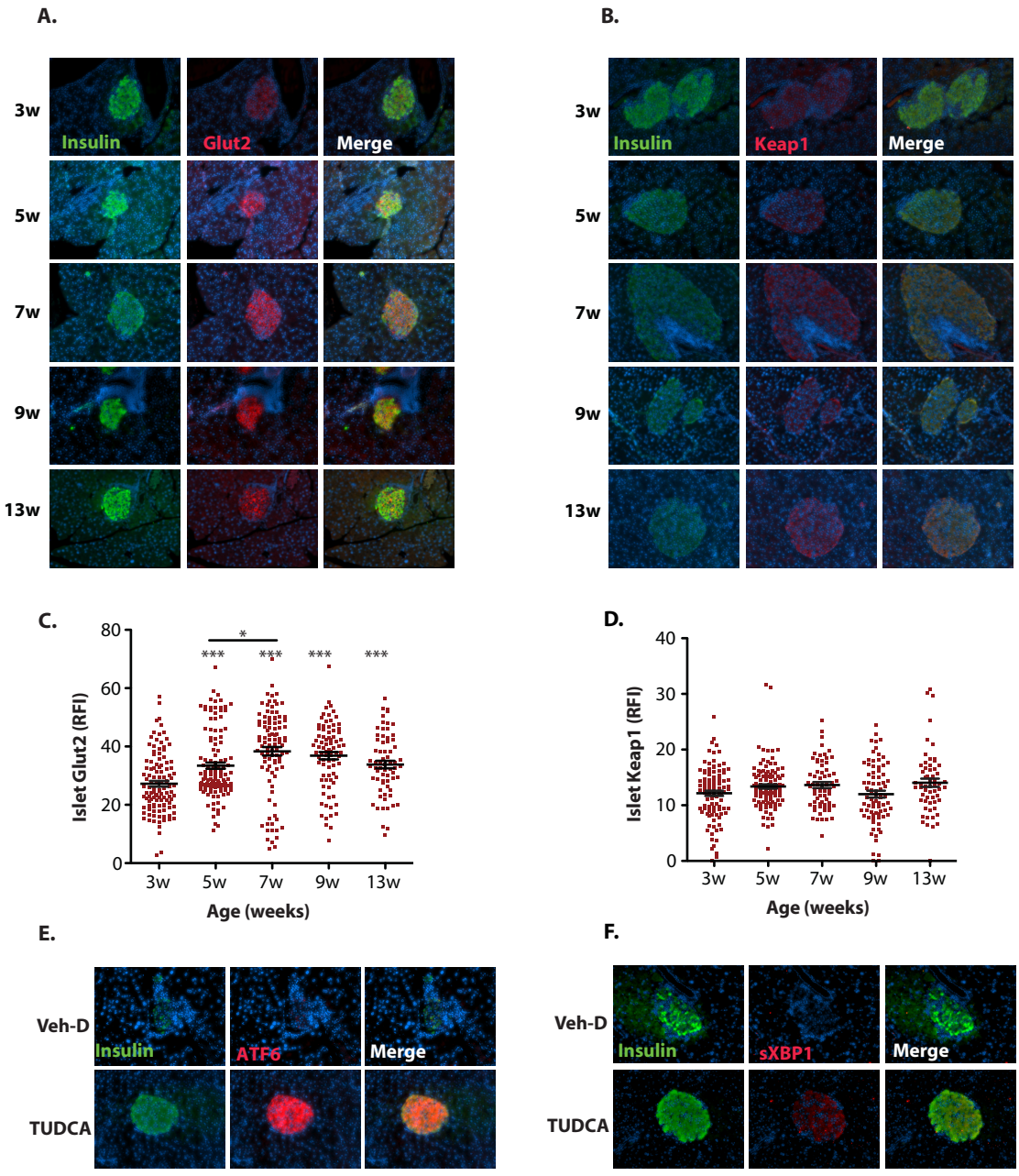

Fig. S2. Specific alterations of Glut2 and Keap1 expression in the islets of NOD mice. A. Pancreatic sections from female NOD mice (*n*=14 for each group) were sacrificed at indicated time points and pancreatic sections were stained with anti-Glut2 (red) or **B.** anti-Keap1 (red) and anti-insulin (green) antibodies. The

cell nuclei were counterstained with DAPI (blue). Quantification of relative fluorescence intensity (RFI) for **C.** Glut2, **D.** Keap1 was done using MATLAB® (20-30 islets/animal/time point). Pancreatic sections of vehicle-treated diabetic (upper panel) or TUDCA-treated RIP-LCMV-GP mice co-stained with anti-Insulin (green) and **E.** anti-ATF6 (red) or **F.** anti-sXBP1 (red) antibodies. The cell nuclei were counterstained with DAPI (blue). All data are represented as mean ± SEM, with statistical analysis performed by one-way ANOVA (****P<0.001*, **P<0.05*).

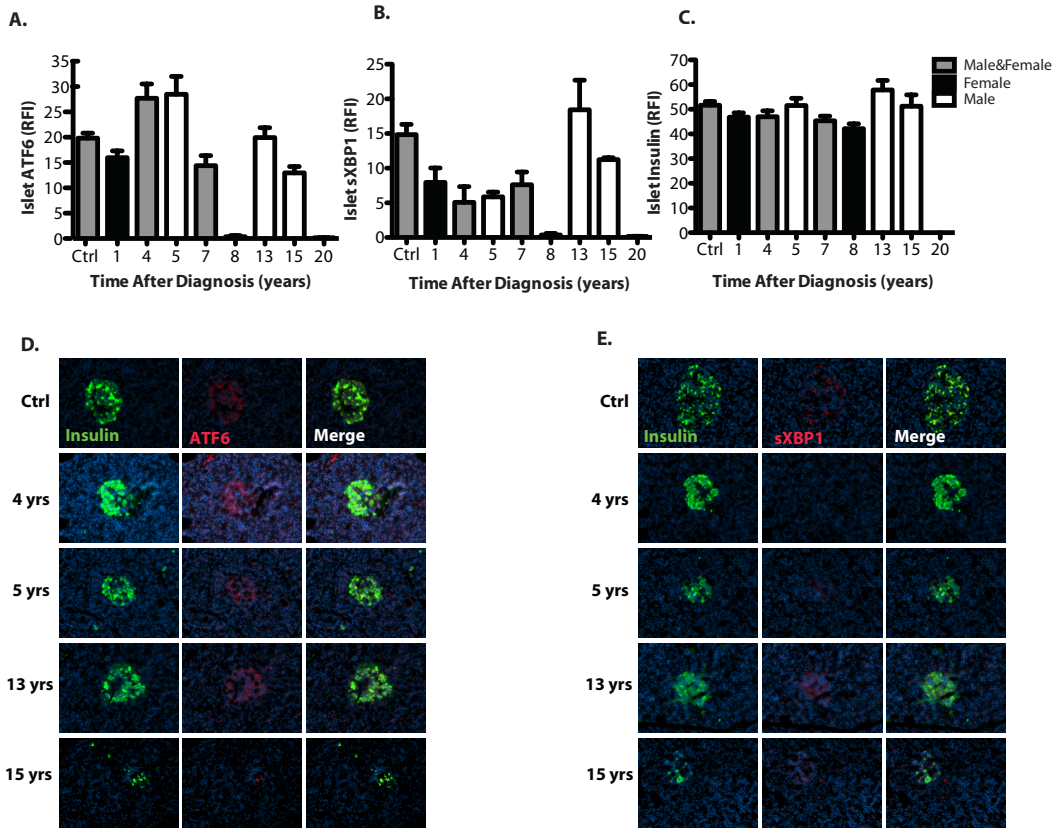

Fig. S3. Dysregulation of molecules critical in the UPR in the islets of male T1D diabetes patients. Pancreas sections from non-diabetic (Ctrl) and diabetic patients that were grouped according to time of the diagnosis (indicated by years) and co-stained either with anti-ATF6 (red), and anti-insulin (green) antibodies, or with anti-sXBP1 (red) and anti-insulin (green) antibodies. Quantification of relative fluorescence intensity (RFI) of **A.** ATF6, **B.** sXBP1 and

C. insulin in the pancreatic sections was calculated on 10-20 islets per time point. Glucagon co-staining was used to determine the islet area for the patient with 20 yrs of diabetes due to complete lack of insulin staining in these islets. The black and white bars indicate female and male subjects respectively. The gray bars indicate the combined results from female and male subjects. **D.** Pancreas sections from non-diabetic (ctrl) and diabetic male patients that were grouped according to time of the diagnosis of diabetes (indicated in years) and co-stained either with anti-ATF6 (red), and anti-insulin (green) antibodies, or **E.** with anti-sXBP1 (red) and anti-insulin (green) antibodies. The cell nuclei were counterstained with DAPI (blue).

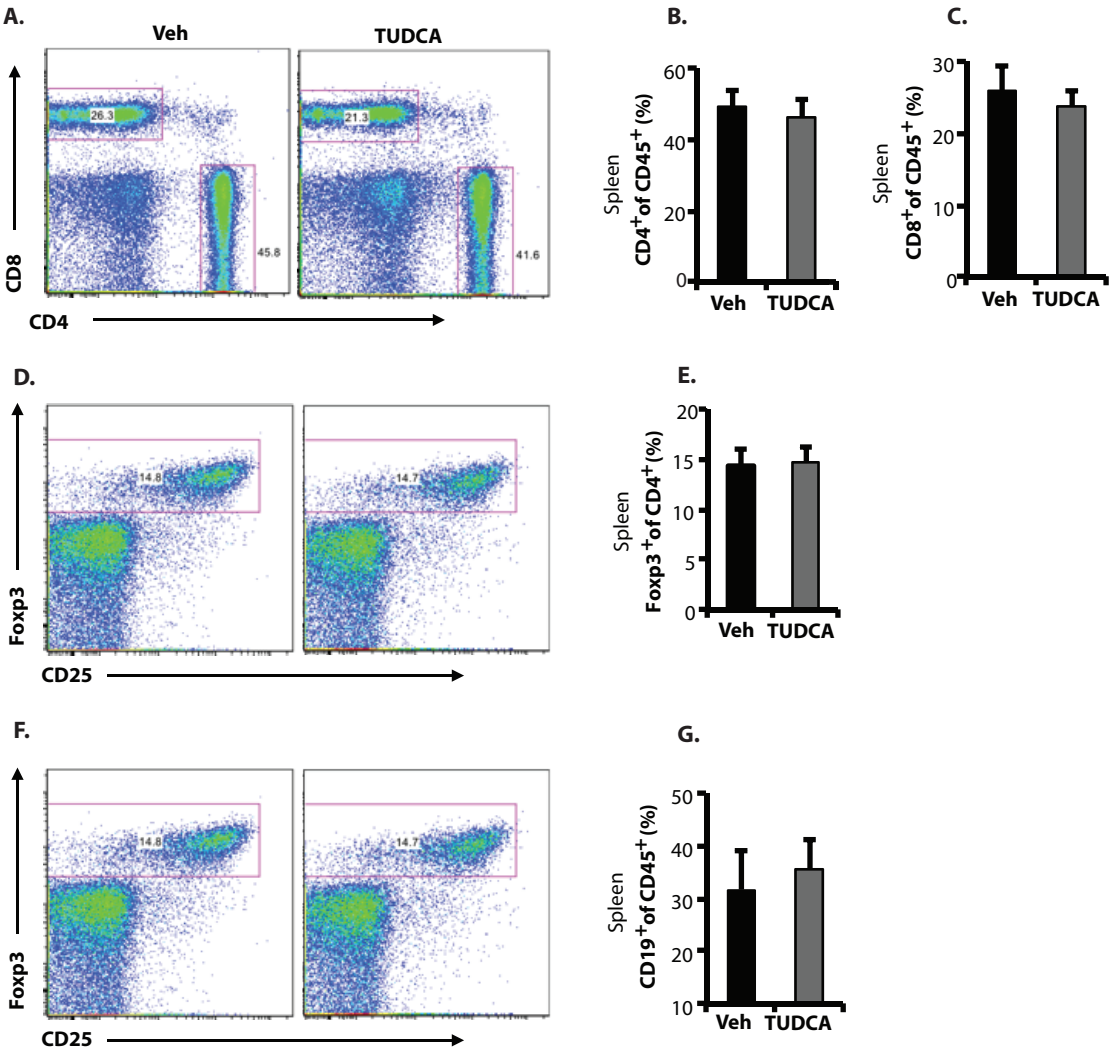

Fig. S4. Immunophenotyping of splenocytes of NOD mice after TUDCA treatment. Age-matched female NOD mice were treated with TUDCA (500 mg/kd/day) or PBS respectively (n=7 in each group). Spleens were dispersed, and cells analyzed by flow cytometry after staining with antibodies recognizing: CD45, CD4, CD8, CD19, CD25 and FoxP3. **A-C.** Cells were pre-gated as CD45+ and fractions of $CD4^+$ and $CD8^+$ T cells were shown in representative plots (left) and quantified (right). **D.** Cells were stained for Foxp3 and CD25 and pre-gated as $CD4^+$ Representative plots were shown and quantified in **E.** **F.**

Similar to (a) except for gating on $CD19^+$ B cells. **G.** Indicates quantification of (f). Student's *t* test did not show any significant statistical difference between vehicle- and TUDCA-treated cells.

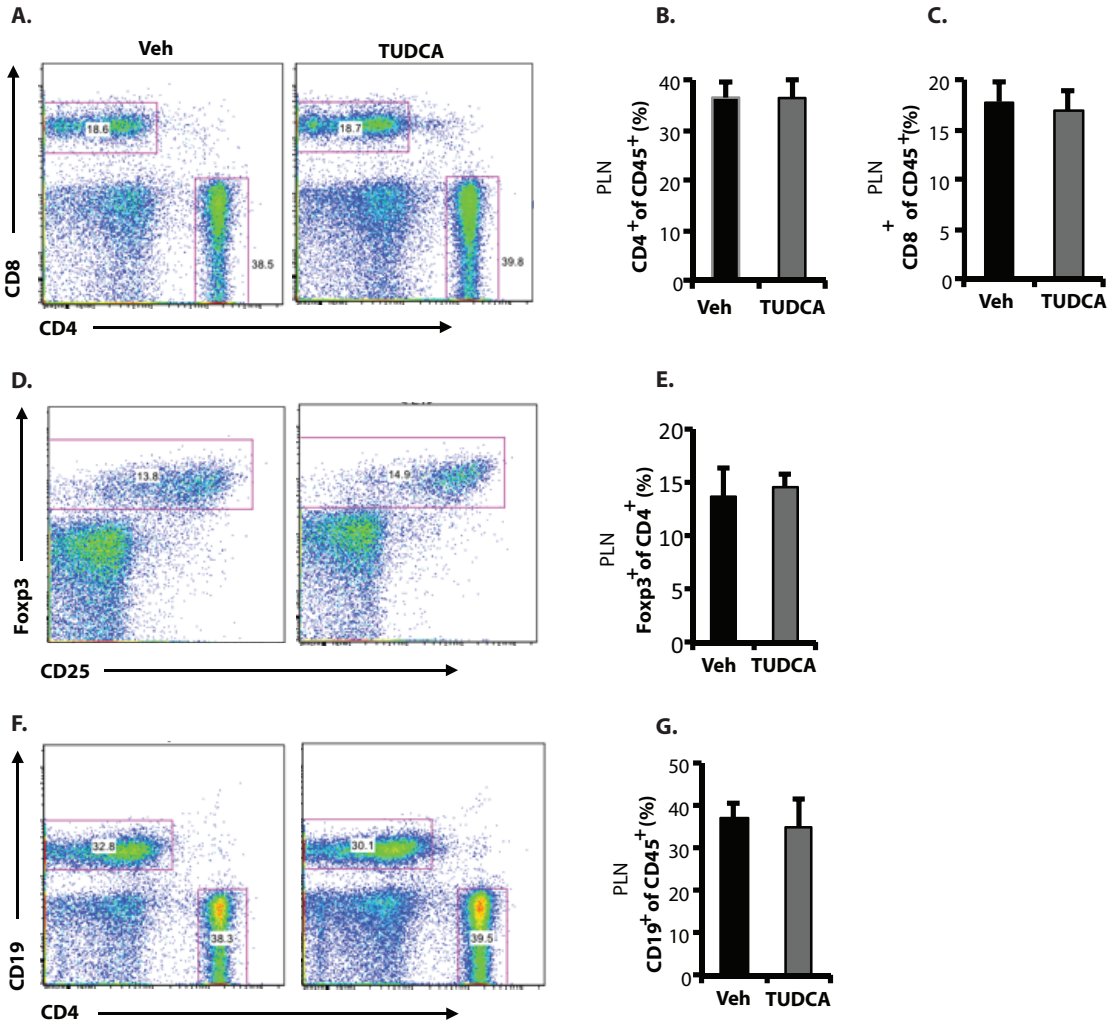

Fig. S5. Immunophenotyping of pancreatic lymph nodes of NOD mice after TUDCA treatment. Age-matched female NOD mice were treated with TUDCA (500 mg/kd/day) or PBS respectively (*n*=7 in each group). Pancreatic lymph nodes (PLN) were dispersed, and cells analyzed by flow cytometry after staining with antibodies recognizing: CD45, CD4, CD8, CD19, CD25 and FoxP3. **A-C.** Cells were pre-gated as CD45+ and fractions of $CD4^+$ and $CD8^+$ T cells were

shown in representative plots (left) and quantified (right). **D.** Cells were stained for Foxp3 and CD25 and pre-gated as $CD4^+$ Representative plots were shown and quantified in **E. F.** Similar to (a) except for gating on $CD19^+$ B cells. **G.** Indicates quantification of (f). Student's *t* test did not show any significant statistical difference between vehicle- and TUDCA-treated cells.

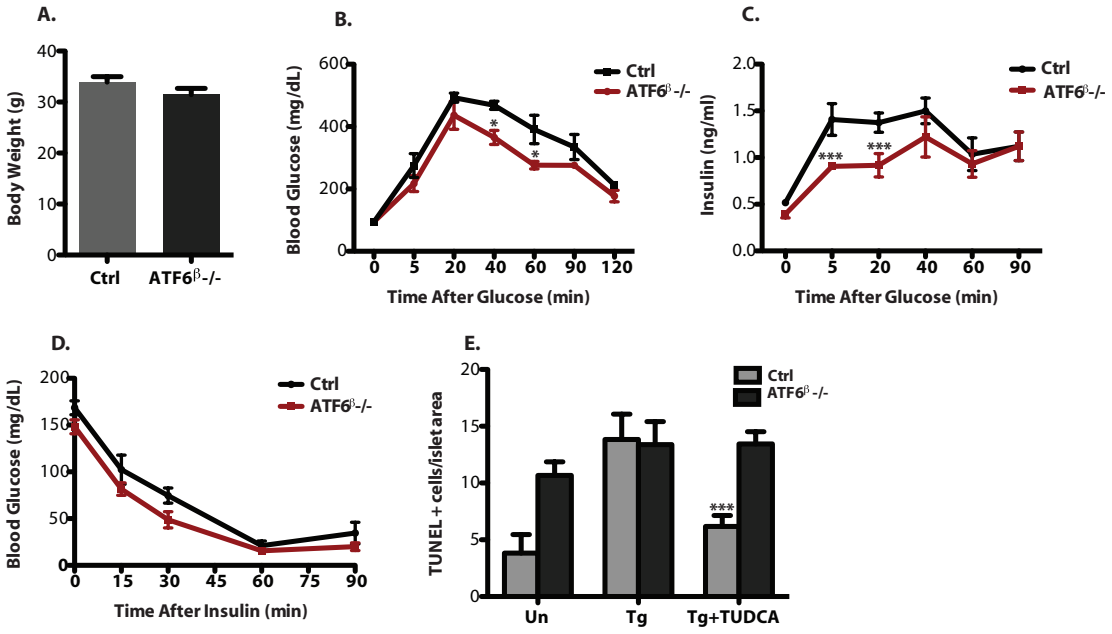

Fig. S6. Deletion of ATF6 branch of the UPR in β cells in vivo. **A.** Body weight measurement of 18 week-old control and $ATF6^{\beta}$-/- male mice. **B.** Glucose tolerance test (GTT) was performed in control and $ATF6^{\beta}$ -/- male mice (*n*=8). **C.** Glucose stimulated insulin secretion (*GSIS)* test *in vivo* using 18-week-old male control and mice $ATF6^{\beta}$ -/- male revealed a mild decrease in *GSIS* in knockout mice compared to the controls. **D.** Insulin tolerance test (ITT) was performed in control and $ATF6^{\beta}$ -/- male mice (*n*=8). **E.** Primary islets were isolated from control and $ATF6^{\beta}$ -/- mice and treated with 2 μM thapsigargin for 24 hours with

or without 500 μM TUDCA. Apoptosis was determined by TUNEL assay. Data are represented as mean ± SEM, with statistical analysis performed by repeated measures two-way ANOVA, or by Student's *t* test (****P<0.001*, **P<0.05*).